

INTERNATIONAL SOCIETY FOR SOIL MECHANICS AND GEOTECHNICAL ENGINEERING



This paper was downloaded from the Online Library of the International Society for Soil Mechanics and Geotechnical Engineering (ISSMGE). The library is available here:

<https://www.issmge.org/publications/online-library>

This is an open-access database that archives thousands of papers published under the Auspices of the ISSMGE and maintained by the Innovation and Development Committee of ISSMGE.

Bearing capacity of strip footing on cohesionless soil under inclined eccentric load

Capacite portante de fondation sur le sol sans cohesion chargeé par la force eccentricue inclinée

V.G. Fedorovsky & N.V. Vorob'ev
 Soil mechanics laboratory, NIIOSP, Moscow, Russia

ABSTRACT

Exact solutions for bearing capacity of heavy cohesionless Coulomb soil base under strip footing are presented. Based on these solutions load inclination and eccentricity influence is analyzed

RÉSUMÉ

Le solution exact pour capacite portant de sol lourd de Coulomb sans cohesion sous fondation sont presente. Avec ses solution l'influence de charge inclinasion et eccentricite est analyseé

1 INTRODUCTION. BOUSSINESQ AND KÖTTER EQUATIONS

The paper describes a solution of the problem for stability of a plate on cohesionless soil base (i.e., soil base, whose material features non-zero weight and the angle of internal friction and zero cohesion). This solution generalizes the known Lundgren-Mortensen (1953) solution in the same sense as the solution (Fedorovsky, 1989, 2003) generalizes Prandtl (1920) solution for the case of weightless cohesive soil base.

The required mathematical tools for solving this problem are Kötter equation for stresses along slip-line and Boussinesq equations for cohesionless wedge limit equilibrium. Below is given a short theoretical overview necessary for further discussion. Consider a cohesionless semi-plane ($z \geq 0$) (a special case of the wedge) with horizontal boundary ($x \geq 0$), whose second half is subjected to a load with triangular distribution, inclined at an angle δ to the normal (Fig. 1a). It is convenient to conduct the analysis in polar coordinate system $\{r, \theta\}$, where θ is the angle counted counterclockwise from the vertical (Fig. 1a).

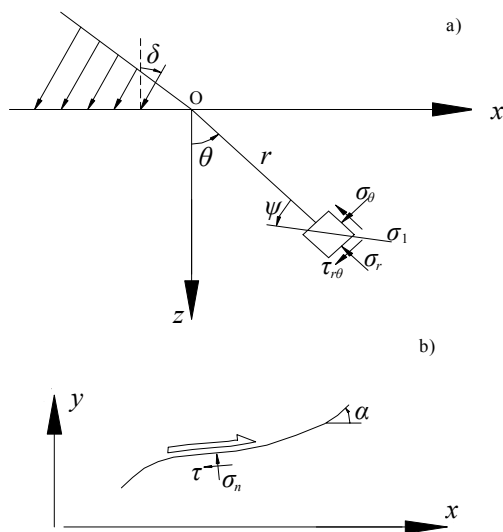


Fig. 1. To the derivation of Boussinesq (a) and Kötter (b) equations

The following expressions can be obtained for stresses in a wedge in limit stress state with the help of Mohr circle:

$$\begin{aligned}\sigma_r &= \sigma(1 + \sin\varphi \cos 2\psi) \\ \sigma_\theta &= \sigma(1 - \sin\varphi \cos 2\psi) \\ \tau_{r,\theta} &= \sigma \sin\varphi \sin 2\psi\end{aligned}\quad (1)$$

where σ is a mean stress at a given point, φ is an angle of internal friction, ψ is an angle between the major principal stress direction and polar radius (Fig. 1a). Boussinesq substitution

$$\sigma = \gamma r S(\theta) \quad (2)$$

where γ is a material specific gravity, reduces the stress state problem in half-plane to finding two unknown functions S and ψ of one variable θ . Substitution (1) and (2) in equilibrium equations yields a system of ordinary differential equations, named Boussinesq equations:

$$\begin{aligned}\frac{dS}{d\theta} &= \frac{S \sin 2\psi - \sin(2\psi + \theta)}{\cos 2\psi - \sin\varphi} \\ \frac{d\psi}{d\theta} + 1 &= \frac{\cos\theta - \sin\varphi \cos(2\psi + \theta) - S \cos^2\varphi}{2S \sin\varphi (\cos 2\psi - \sin\varphi)}\end{aligned}\quad (3)$$

Solutions of this system of equations (see Fedorovsky & Vorob'ev, 2001, for details), corresponding to maximum (passive) pressure applied to soil base, can be presented as $S_b(\alpha, \delta)$, $\psi_b(\alpha, \delta)$ and $\rho_b(\alpha, \delta)$. Here $\alpha = \pi/2 + \theta$ is the angle, counted from the loaded surface; $\rho(\alpha)$ is the slip-line equation in polar coordinates, obtained by integrating the following differential equation:

$$\frac{d\rho}{d\alpha} = \frac{\rho}{\tan(\psi - \mu)} \quad (4)$$

with initial condition $\rho(0) = 1$; $\mu = \pi/4 - \varphi/2$. Note that this is not the "active" slip-line along which occurs maximum shear and to which the rupture-line corresponds in Prandtl type solutions, but the conjugated one.

These functions play a key role in the method, described below, for calculating bearing capacity of cohesionless soil under a plate. Also note that the functions are parametrically dependent on the load inclination angle δ , to which contact friction angle corresponds, defined by plate bottom roughness.

Besides, this study employs the fact that for an arbitrary slip-line normal $\sigma_n = \sigma \cos^2 \varphi$ and shear stresses $\tau = \sigma_n \tan \varphi$ comply with Kötter equation, which for the "left-side" mutual soil displacement (Fig. 1b) have the following form (Fedorovsky, 1987)

$$\frac{d\sigma_n}{dx} + 2\tau \frac{d\alpha}{dx} + \gamma \frac{\sin(\alpha + \varphi) \cos \varphi}{\cos \alpha} = 0 \quad (5)$$

Here $\alpha = \arctan(dy/dx)$. This equation has a confined analytical solution for slip-lines, having the form of logarithmic helices or straight lines, given below.

2 THE TWO-SIDED BEARING CAPACITY PROBLEM

Consider a strip footing on cohesionless soil base. The failure zone deviates from Ludgren-Mortensen (1953) scheme due to symmetry loss connected with transition from the central vertical to the eccentric and/or inclined loading of the plate.

According to the proposed scheme the plate bottom rests on a non-deformable triangle core $B_1C_1B_2$, limited by a curvilinear slip-line B_1C_1 on the right, and by a combined curvilinear slip-line $B_2C_2C_1$ on the left (Fig. 2). Upthrust zones $B_1C_1D_1E_1A_1$ and $B_2C_2D_2E_2A_2$ adjoin the core and the plate bottom (Figs. 2b,c don't show these zones). Plate bottom A_1A_2 , having width b , is divided into three portions i.e., the central one B_1B_2 , where the plate is coupled with the stiff core, and two side ones A_1B_1 and A_2B_2 , having widths b_1 and b_2 respectively, where the upthrust soil slips along the plate bottom. The friction along the bottom is directed away from the plate symmetry axis, and the friction ratio is equal to $\tan \varphi_a$, where φ_a is angle of contact friction ($0 \leq \varphi_a \leq \varphi$). Zones $A_1D_1E_1$ and $A_2D_2E_2$ feature maximum Rankine limit stress state while zones $B_1C_1D_1A_1$ and $B_2C_2D_2A_2$ have the Boussinesq one (see above). Isolated slip-line C_1C_2 , dividing the stiff core and the stiff massif of static soil, can only be (based on kinematic permissibility for the medium, following plastic flow law, associated with the Coulomb condition) a logarithmic helix with its center at point O (Fig. 2a,b) or a straight line (Fig. 2c).

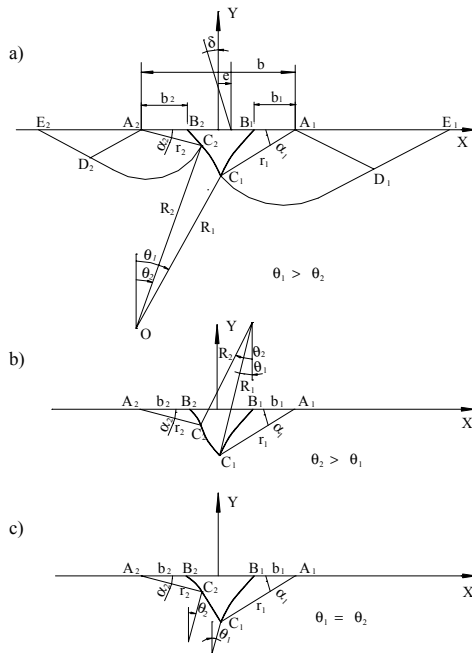


Fig. 2. Solution schemes for two-sided case

Due to loss of stability i.e., when the load P , applied to the plate, inclined at angle δ with eccentricity e (Fig. 2a), reaches the limit value, the plate movement along with the core is clockwise rotation about point O (Fig. 2a) or counterclockwise rotation (Fig. 2b) or translation at angle φ to line C_1C_2 (Fig. 2c).

Let us determine the main elements of stress state and geometry at point C_1 (the core apex). In view of the above statements at this point

$$\begin{aligned} r_1 &= b_1 \rho_b(\alpha_1; \varphi_a) = b_1 \rho_1 \\ \sigma_1 &= \gamma r_1 S_b(\alpha_1; \varphi_a) = \gamma b_1 \rho_1 S_1 \\ \psi_1 &= \psi_b(\alpha_1; \varphi_a) \end{aligned} \quad (6)$$

where σ_1 is mean stress at point C_1 , ψ_1 is angle between the major principal stress and radius A_1C_1 ; geometric parameters r_1 and α_1 are shown on Fig. 2; functions ρ_b , S_b and ψ_b are defined above. The angle between the tangent line to the slip-line B_1C_1 at point C_1 and the vertical

$$\theta_1 = \pi/2 - \alpha_1 - \psi_1 + \mu \quad (7)$$

Radius of the logarithmic helix C_1C_2 . $OC_1 = R_1$ belongs to this tangent line. The angle between the radius and the helix at each point is equal to $\pi/2 - \varphi$. The second radius $R_2 = OC_2$ is inclined to the vertical at angle

$$\theta_2 = -\pi/2 + \alpha_2 + \psi_2 + \mu, \quad (8)$$

where ψ_2 and other stress state parameters can be found with the help of formulae (6) after substitution of all indices 2 for 1. For convenience of presentation of relationships along the logarithmic helix introduce index

$$m = \text{sign}(\theta_1 - \theta_2) \quad (9)$$

The case $m = 1$ corresponds to Fig. 2a, $m = -1$ to Fig 2b; $m = 0$ to Fig. 2c. Therefrom, at an arbitrary point of helix in polar coordinates $\{R, \theta\}$ with the center at point O

$$R = R_s \exp[-(\theta - \theta_s) \tan \varphi], \quad (10)$$

where R_s is the radius, corresponding to an angle θ_s . Kötter equation along this helix has the following solution:

$$\begin{aligned} \sigma(\theta) &= \left[\sigma_s + \gamma m R_s \frac{\cos \Psi \cos(\theta_s - \Psi)}{\cos^2 \varphi} \right] \exp[2(\theta - \theta_s) \tan \varphi] \\ &- \gamma m R_s \frac{\cos \Psi \cos(\theta - \Psi)}{\cos^2 \varphi} \exp[-(\theta - \theta_s) \tan \varphi] \end{aligned} \quad (11)$$

Here σ_s is the mean stress at point $\theta = \theta_s$; $\Psi = \arctan(3 \tan \varphi)$.

In order to find the problem solution for given α_1 and α_2 one should satisfy the following three conditions (two geometric and one stress-related)

$$\begin{aligned} b &= x_{A1} - x_{A2} = r_2 \cos \alpha_2 - m R_2 \sin \theta_2 + m R_1 \sin \theta_1 + r_1 \cos \alpha_1 \\ 0 &= y_{A1} - y_{A2} = -r_2 \sin \alpha_2 - m R_2 \cos \theta_2 + m R_1 \cos \theta_1 + r_1 \sin \alpha_1 \\ \sigma_2 - \sigma_1 &= \sigma(\theta_2) - \sigma(\theta_1) \end{aligned} \quad (12)$$

After substituting expressions (6) for r_i and σ_i and expressions (10) and (11) for R_i , and $\sigma(\theta_i)$, respectively, with $\theta_s = \theta_2$ (i.e., $R_s = R_2$) we obtain a system of three linear equations with respect to b_1 , b_2 and R_2 .

$$\begin{aligned} b_1 \rho_1 \cos \alpha_1 + b_2 \rho_2 \cos \alpha_2 + m R_2 (\lambda \sin \theta_1 - \sin \theta_2) &= b \\ b_1 \rho_1 \sin \alpha_1 - b_2 \rho_2 \sin \alpha_2 + m R_2 (\lambda \cos \theta_1 - \cos \theta_2) &= 0 \\ \gamma b_1 \rho_1 S_1 - \frac{\gamma b_2 \rho_2 S_2}{\lambda^2} - \gamma m R_2 \frac{\cos \Psi}{\cos^2 \varphi} \left[\frac{\cos(\theta_2 - \Psi)}{\lambda^2} - \lambda \cos(\theta_1 - \Psi) \right] &= 0 \end{aligned} \quad (13)$$

Here notation $\lambda = \exp[(\theta_2 - \theta_1) \tan \varphi]$ is introduced.

The solution of system (18) shall comply with conditions $b_1 > 0$; $b_2 \geq 0$; $R_2 > 0$. If at least one of these conditions is vio-

lated the solution is physically impossible i.e., for a given set of input parameters solution $\{\alpha_1, \alpha_2\}$ is non-existent.

In the case of $m = 0$ (Fig. 2c) the logarithmic helix degenerates into straight line C_1C_2 , whose inclination angle ξ to horizontal line, counted clockwise, is equal to $\theta + \varphi$, where $\theta = \theta_1 = \theta_2$. The Kötter integral along a straight line has the following form:

$$\sigma = \sigma_s + \gamma(x - x_s) \frac{\sin(\xi - \varphi)}{\cos\varphi \cos\xi} = \sigma_s + \gamma(x - x_s) \frac{\sin\theta}{\cos\varphi \cos(\theta + \varphi)} \quad (14)$$

By introducing $d_{12} = C_1C_2$ and performing transformations similar to those done to obtain (13) we get a system of three linear equations with respect to b_1, b_2 and d_{12} .

$$\begin{aligned} b_1\rho_1 \cos\alpha_1 + b_2\rho_2 \cos\alpha_2 + d_{12} \cos(\theta + \varphi) &= b \\ b_1\rho_1 \sin\alpha_1 - b_2\rho_2 \sin\alpha_2 - d_{12} \sin(\theta + \varphi) &= 0 \\ \gamma b_1\rho_1 S_1 - \gamma b_2\rho_2 S_2 - \gamma d_{12} \sin\theta / \cos\varphi &= 0 \end{aligned} \quad (15)$$

Solution (15) admissibility conditions are $b_1 > 0; b_2 \geq 0; d_{12} \geq 0$, as before they have an evident physical sense.

After the geometry of the solution is found for given α_i and α_2 , parameters of the failure load can be derived. They can be obtained from the equilibrium condition of curvilinear quadrangle $A_1C_1C_2A_2$. Along straight lines A_iC_i ($i = 1, 2$) the normal and shear stress profiles are triangular (with zeroes at apexes A_i) and can be found from Boussinesq stress presentation (1). Namely

$$\begin{aligned} \sigma_n &= \gamma r S_i (1 - \sin\varphi \cos 2\psi_i) \\ \tau &= \gamma r S_i \sin\varphi \sin 2\psi_i \end{aligned} \quad (16)$$

Here r is distance from apex A_i .

Stresses along the segment of slip-line C_1C_2 can be found by means of formulae

$$\sigma_n = \sigma \cos^2\varphi \quad \tau = \sigma_n \tan\varphi \quad (17)$$

where σ is calculated by formula (11) (with $m \neq 0$) or (15) (with $m = 0$). Integrals along this segment can be calculated analytically, including the one for the soil weight, and along intervals A_iC_i .

Equilibrium conditions of $A_1C_1C_2A_2$ yield vertical V and horizontal H components of ultimate load P , applied to the plate, and also its moment M_0 with respect to the origin of coordinates, located in the plate center.

Then load inclination and eccentricity can be found

$$\delta = \arctan(H/V) \quad e = M_0/V \quad (18)$$

Having returned to Lungren-Mortensen solution, note its two basic differences for the proposed one. Firstly, the preceding solution relates to just the case of $\alpha_1 = \alpha_2$, and points C_1 and C_2 coincide. This is the case of central vertical load. The proposed solution enables independent variation of δ and e (these two parameters are related to two independent parameters of α_1 and α_2). Secondly, Lungren & Mortensen consider just the case of perfectly rough plate bottom i.e., $\varphi_a = \varphi$. Here any contact friction angle is possible.

Consider the case of two-sided upthrust with the plate that lost stability moving to the right, which fact explains the solution asymmetry. If the plate moves to the left the whole system shall be mirrored about central axis $x = 0$. In the general case consider two variants and select the smaller of the ultimate load values. In fact, it means that in the case of right-side upthrust only solutions for $\delta \geq 0$ have a physical sense.

3 THE ONE-SIDED BEARING CAPACITY PROBLEM

One-sided upthrust case has a major practical significance. It realizes, for example, when the soil base is surcharged, e.g. to the left from the plate (Fig. 3). In this case the problem is somewhat simpler. The solution parameters are α_1 and θ_2 . And again, depending on the sign of difference $\theta_1 - \theta_2$ there are three possible solutions (Fig. 3 a,b,c). An essential difference from the two-sided upthrust is that σ_2 is not equal to 0 at the given back point of the plate. In case of $m \neq 0$ the following analogue of the system of equations (18) may be obtained with respect to unknowns b_1, σ_2 and R_2

$$\begin{aligned} b_1\rho_1 \cos\alpha_1 + mR_2(\lambda \sin\theta_1 - \sin\theta_2) &= b \\ b_1\rho_1 \sin\alpha_1 + mR_2(\lambda \cos\theta_1 - \cos\theta_2) &= 0 \\ \gamma b_1\rho_1 S_1 - \frac{\sigma_2}{\lambda^2} - \gamma m R_2 \frac{\cos\Psi}{\cos^2\varphi} \left[\frac{\cos(\theta_2 - \Psi)}{\lambda^2} - \lambda \cos(\theta_1 - \Psi) \right] &= 0 \end{aligned} \quad (19)$$

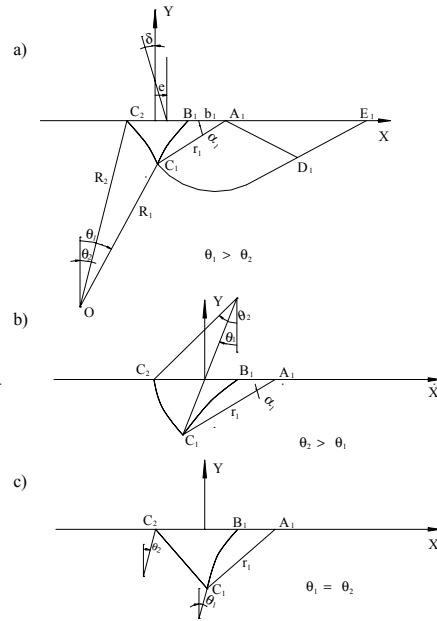


Fig. 3. Solution schemes for one-sided upthrust case

If $m = 0$ unknowns b_1, σ_2 and $d_{12} = C_1C_2$ then the solution of the system of equations (analogue of (15))

$$\begin{aligned} b_1\rho_1 \cos\alpha_1 + d_{12} \cos(\theta + \varphi) &= b \\ b_1\rho_1 \sin\alpha_1 - d_{12} \sin(\theta + \varphi) &= 0 \\ \gamma b_1\rho_1 S_1 - \sigma_2 - \gamma d_{12} \sin\theta / \cos\varphi &= 0 \end{aligned} \quad (20)$$

Parameters of the ultimate load can be found from the equilibrium equations of, generally speaking, curvilinear triangle $A_1C_1C_2$ i.e., as compared with the previous case there is no integration over A_2C_2 . Limitation of the solutions include both the previous ones ($b_1 > 0, R_2 > 0$ or $d_{12} \geq 0$) and the new ones ($\sigma_2 \geq 0, \mu - (\omega_a + \varphi_a)/2 \leq \theta_2 \leq \mu + (\omega_a + \varphi_a)/2$). Here $\omega_a = \arcsin(\sin\varphi_a / \sin\varphi)$.

The last pair of inequalities means limitation of the absolute value of ratio (τ/σ_n) along the plate bottom at corner point C_2 by the value $\tan\varphi_a$.

4 RESULTS AND CONCLUSIONS

The proposed solution can not be obtained directly (for the given eccentricity e_0 and the load inclination δ_0), but parametrically for parameters α_1 and α_2 (or θ_2). The total family of solutions for all potential combinations of these parameters covers a

certain area of plane $\{e, \delta\}$. Beside the above limitations, in case of $m = -1$, solutions for both cases are neglected, in which the kinematically imposed (see Fedorovsky, 2003) inequality is not fulfilled for the rotation center

$$x_0 + y_0 \tan \varphi \geq 0,5b - b_1 \quad (21)$$

With fixed angle δ the point, when this inequality becomes equality, corresponds to the achievement of minimally possible load eccentricity e_{min} while the maximally possible eccentricity e_{max} is achieved if $\alpha_2 = 0$ (two-sided upthrust) or $\theta_2 = \mu - (\alpha_1 + \varphi_a)/2$ (one-sided upthrust). If the eccentricity exceeds the allowable limits then a part of the plate disrupts from the soil base surface in such a way that in remaining portion the required maximum (or minimum) eccentricity is preserved. The ultimate load is then calculated with the help of formula (Fedorovsky, 1989)

$$V(e) = \begin{cases} V(e_{max}) \left(\frac{b - 2e}{b - 2e_{max}} \right)^2 & \text{for } e > e_{max} \\ V(e_{min}) \left(\frac{b + 2e}{b + 2e_{min}} \right)^2 & \text{for } e < e_{min} \end{cases} \quad (22)$$

Notably, in the one-sided case with $e > e_{max}$ the separation of the plate from soil occurs in the rear and the one-sided upthrust becomes two-sided. However, there occurs no jump, because at this moment both solutions coincide, as is seen on Fig. 4. This figure shows dependences $V(e)$ with $\delta = 0$ and 5° for two-sided upthrust (solid line) and one-sided upthrust (dotted lines) for $\varphi = \varphi_a = 30^\circ$. Notice that graph $V(e)$ for $\delta = 0$ and $e < 0$ for two-sided case correspond to leftward motion.

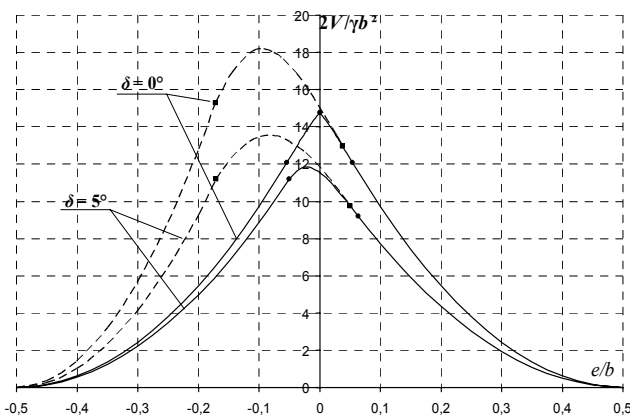


Fig. 4. Dependence of bearing capacity on load eccentricity for two inclination angles. The points mark boundaries between zones of existence of solution without separation zones (ultimate eccentricities):

● — two-sided case; - - - ■ - one-sided case

Fig 5 shows isolines of bearing capacity $2V/\gamma b^2$ for $\varphi = \varphi_a = 30^\circ$. For the case of two-sided upthrust the solution is given just for positive inclination angles while the negative solution is symmetrical. For one-sided upthrust the solution for $e > e_{max}$ does not exist. For fixed inclination angle δ the maximum bearing capacity is achieved for the eccentricity e , which corresponds to $m = 0$ case i.e., to the plate displacement without rotation (Fig. 2c, 3c).

Table 1. Soil base bearing capacity $2V/\gamma b^2$ for vertically and centrally loaded plate and $\varphi = 30^\circ$

$\varphi_a,^\circ$	0	5	10	15	20	25	30
Two-sided	7.65**	9.87	11.75	13.14	14.03	14.61	14.75*
One-sided	-	-	-	13.90	14.57	14.91	15.50

Consider other cases of $\varphi = 30^\circ$. If $e = \delta = 0$ (vertical central load) Table 1 gives values $N_\gamma = 2V/\gamma b^2$ for various values φ_a . Evidently, bearing capacity for the case of one-sided upthrust is somewhat greater, but for this case and small φ_a the solution does not exist (blanks in Table 1). If $\varphi_a = 0$ and the thrust is one-sided then the core degrades to one point and the failure follows the Hill case.

Lundgren and Mortensen (1953) analyzed the unique case of two-sided upthrust conditions, marked with asterisk in the Table, and the solution coincides with those given in Table 1. One more exact solution was given by Malyshev (1994). It relates to two-sided upthrust for a perfectly smooth plate, for which Hill solution is valid. Herein, the numerical result also coincides with the one given in Table 1 (marked with two asterisks).

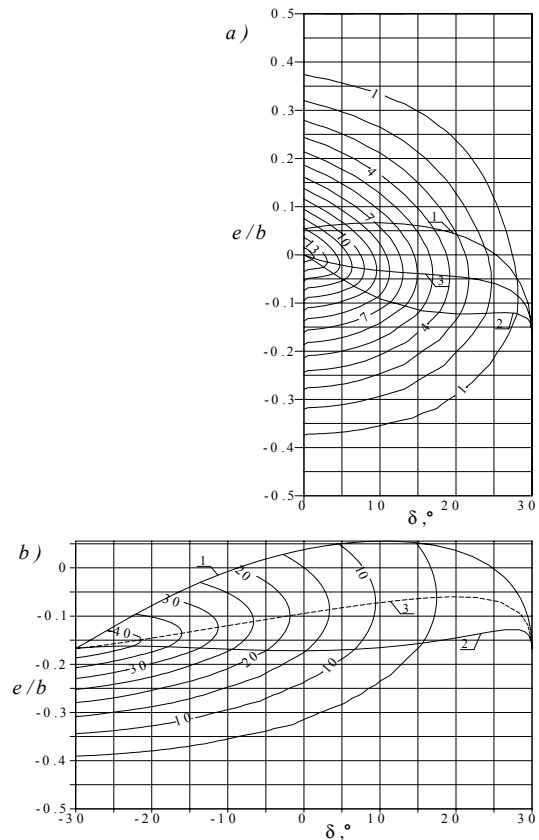


Fig. 5. Isolines of bearing capacity for two-sided (a) and one-sided (b) upthrust. Also lines e_{max} (1), e_{min} (2) and $m = 0$ (3) are shown.

In conclusion we would like to stress that the obtained exact solution is essentially different as to the form and dimensions of upthrust zones from the similar solution for weightless cohesive soil base that makes the three-member Terzaghi formula inaccurate in principle.

REFERENCES

- Fedorovsky V.G. 1989. Stability of foundations under eccentric and inclined loads. *Proc. 12th ICSMFE*, v.2, Rio-de-Janeiro, 421-425
- Fedorovsky V.G. 2003. Bearing capacity of an eccentrically and obliquely loaded strip foundation on a weightless cohesive bed. *Soil Mechanics and Foundation Engineering*, №5, 161-172
- Fedorovsky V.G. 1987. Kötter equation for anisotropic and nonhomogeneous soils. *Proc. NIIOSP*, №88 (in Russian)
- Fedorovsky V.G., Vorob'ev N.V. 2001. Limit equilibrium of cohesionless wedge and coefficients of active and passive pressure. *Trans. VNIIG*, № 239 (in Russian)
- Lundgren H., Mortensen K. 1953. Determination by the theory of plasticity of the bearing capacity of continuous footings on sand. *Proc. 3rd ICSMFE*, v.1, Zurich, 409-412
- Malyshev M.V. 1994. *Soil strength and stability of foundations*. Stroyizdat, Moscow (in Russian)
- Prandtl L. 1920. Über die Härte plastischer Körper. *Nachr. d. Ges. d. Wiss., math.-phys. Kl.*, Göttingen, 74-79